Editorial Manager(tm) for Food Biophysics
Manuscript Draft

Manuscript Number:

Title: Application of high intensity ultrasounds to control the size of whey proteins particles

Article Type: Original Research

Keywords: microparticles; ultrasounds; protein aggregates; fat mimetic

Corresponding Author: Dr. Ana M. R. Pilosof,

Corresponding Author's Institution: Facultad de Ciencias Exactas y Naturales, Universidad de Buenos Aires

First Author: Laura Gordon, Food Science and Technology

Order of Authors: Laura Gordon, Food Science and Technology; Ana M. R. Pilosof

Suggested Reviewers: Perla Relkin PhD
Laboratoire de Biophysique-UMR 1211, AgroParisTech -
perla.relkin@agroparistech.fr
Deep knowledge on whey proteins denaturation, aggregation

Dominique Durand PhD
Directeur de Recherche CNRS, Université du Maine
dominique.durand@univ-lemans.fr
Deep knowledge on whey protein aggregation and light sacttering techniques

Mar Villamiel PhD
Instituto de fermentaciones industriales-CSIC-España
ifiv308@ifi.csic.es
Works on ultrasounds on proteins

David J McClements PhD
Umass
mcclements@foodsci.umass.edu
application of ultrasound in food analysis and processing

Maria Cristina Añon PhD
CIDCA, Universidad de La Plata
mca@biol.unlp.edu.ar
Works on food protein functionality

Application of high intensity ultrasounds to control the size of whey proteins particles

Laura Gordon* and Ana.M.R.Pilosof[1]**

[1]Departamento de Industrias, Facultad de Ciencias Exactas y Naturales, Universidad de Buenos Aires, Ciudad Universitaria (1428), Buenos Aires, Argentina.

*Research fellow Universidad de Buenos Aires

** Member Consejo Nacional de Investigaciones Científicas y Técnicas

Corresponding author: A.M.R. Pilosof. Tel: +54 11 45763377; fax: +54 11 45763366.

E-mail address: apilosof@di.fcen.uba.ar

This research was supported by Universidad de Buenos Aires, Agencia Nacional de Promoción Científica y Tecnológica and Consejo Nacional de Investigaciones Científicas y Técnicas de la República Argentina.

Abstract

In this paper we reported a new method to prepare whey protein microparticles via high intensity ultrasound disruption. Particles morphology was characterized by confocal microscopy and their size and distribution were analysed by light scattering technique.

Starting Whey Protein Isolate exhibited changes in size and distribution according to its concentration. For WPI 7.5 % (w/w) mean size was 0.7 µm and upon sonication at ambient temperature the size was reduced up to 0.2 µm showing the particles a rounded morphology. Sonication at room temperature of gelled WPI led to particles with sizes between 0.1 and 10 µm which had a tendency to flocculate. When WPI was submitted to sonication under heating at protein denaturation temperature, different effects were observed according to protein concentration. The particle size was reduced for the lowest WPI concentration (7.5 % wt), did not change at 9 % wt but strongly increased at 12 % wt, in comparison with the untreated sample.

WPI particles of desired size in the micron range may be obtained either by sonication of gelled WPI or by sonication under heating at denaturation temperature, by controlling processing variables.

Keywords: microparticles, ultrasounds, protein aggregates, fat mimetic

Introduction

Within the last ten years new and effective food processing methods have been developed. An alternative technology is high intensity ultrasound (US) involving intensities higher than 1W/cm^2 and frequencies between 16 and 100 kHz [1,2]. The sound energy passes through the medium resulting in a continuous wave-type motion, longitudinal waves will be generated and therefore it will create dynamic agitation and shear stresses of the medium particles [2]. US generate heat and cavitation. Heat is produced by friction between the probe, the medium and the reactor´s walls. Cavitation is the formation and collapse of bubbles, generating extremely high pressures and temperatures in the center of cavitation bubbles. It is considered the main mechanism through which chemical activities in sonochemistry occurs [2,3]. The relation between heat and cavitation is very complex. When liquid´s temperature rises, the number of bubbles increases, so the cavitation should be more intensive. On the other hand, as the temperature rises, liquid has higher vapour pressure, so the gas pressure in the bubbles becomes higher and the implosion force of cavitation decreases. These two opposing tendencies suggest that an optimal temperature might occur at which cavitation is more intensive.

There are also other conditions that affect intensity and energy distribution in bulk like reactor´s geometry, position and shape of the microtip, sample's volume and concentration [4-6].

Many applications of US in food processing are reported, besides the inactivation of microorganisms. It was observed that in a continuous flow of milk the simultaneous application of ultrasound and heat treatment increased denaturation velocity of enzymes, alpha–lactalbumin and beta–lactoglobulin with no changes in the casein [7,8].

US also improve a substantial reduction in fat globule size and a better distribution of them causing a good homogenization [7-9]. US are also useful to create bovine serum albumin in poly (lactic – co – glycolic acid) microspheres. The microspheres exhibited a 15 – 40 µm average diameter and the encapsulation was 70% efficient [10,8]. US can reduce phosphatidilcoline liposomes size from 300 nm to 140 nm [11]. The application of high intensity ultrasound to modify biopolymers is increasingly studied and most works focuse on the ability of ultrasound to depolymerise polysaccharides such as dextran, xanthan, lambda-carrageenan, chitosan, starch and hydroxypropilmethylcellulose [12-18] which impacts on their functional properties, *i.e.*, relative molar mass, molecular weight, depolymerisation, gelation, viscosity. The effects of ultrasound on the degradation of polysaccharides depend on concentration, reaction temperature, nature of solvent and ultrasonic time. Polysaccharides are degraded faster in dilute solutions than in concentrated solutions and faster at lower temperatures than at higher ones[13]. Degradation increases with prolonged ultrasonication time. Generally polysaccharides with higher molecular weight are more easily degraded [19,16]. Modification of proteins by US is less studied. Recently, structural and functional changes in ultrasonicated bovine serum albumin (BSA) have been reported [20].

US can be used for the preparation of nano and micromaterials. It has been applied to prepare tin nanoparticles from bulk tin achieving diameters ranging between 50 – 300 nm depending on the US intensity applied [21]. Also the sonolysis of silica and alumina particles could reduce their diameter following a first order kinetic regime. It was noticed that reduction is faster for larger particles than for the smaller ones [3,22]. In another study it was found that size reduction by ultrasound could be applied to dickite. After 10 hours of sonication (20 kHz and 750 W) it was observed a complete

destruction of the starting book-like structures and most of the broken particles exhibited sizes of less than 5 μm [23].

The aim of the present work was to assess the ability of US to control the size of protein microparticles. Protein microparticles are used as fat replacers because they can mimic one or more sensory and physical functions of fat in food. These fat mimetics are made from milk whey protein or egg protein, and provide from 1kcal/g to 4kcal/g. Microparticulated proteins should have 4 μm or less and be spherical, to provide a creamy mouth feel similar to fat. They often incorporate water and may be useful in amounts less than fat and can be used in dairy products, such as fat-free ice-creams, frozen desserts, and milk shakes; reduced fat versions of butter, sour cream; low fat cheese; yoghurt; low-fat baked goods; salad dressing; margarine; mayonnaise; coffee creamers; soups; and sauces.

Materials and methods

WPI was purchased from Carbery Food Ingredients Ltd. (Ballineen, Co. Cork, Ireland). The protein was purified from sweet whey by microfiltration and ultrafiltration, then it was spray dried. The composition of the powder (dry basis) was 92% protein, 5% moisture, 1.5% fat, lactose (balance to 100%), 4% ash (major components were 0.44% Ca^{2+}, 0.16% Na^{+}, 0.07% Mg^{2+}, 0.13% K^{+}, 0.45% phosphorus, 0.01% Cl^{-}).

Sample preparation

The protein dispersions (7.5, 9, 12 and 15 % wt) were prepared at room temperature with distilled water and pH was adjusted to 7 with NaOH 1N.

Gelation was accomplished by heating WPI dispersions (7.5, 9, 12, 15, 20 % wt) in a dry bath (Thermoline dri – bath, Barmstead, USA) at 80ºC for 30 minutes. The gel was mixed with distilled water at 1/1 ratio before the US treatment in order to increase the efficiency of US. Thus, a 15 % wt WPI gel was sonicated at 7.5 % wt because of dilution with water. All the samples were stored at 4ºC at least for 2 hours before sonication.

High-intensity ultrasound treatment

A high intensity ultrasonic processor (Model VCX 750, Vibra-Cell, Sonics, USA) operating at 20 kHz frequency with a 13mm (1/2 inch) high grade titanium alloy probe threaded to a 3mm tapered microtip was used to sonicate 10 ml of protein sample in a 15 ml glass tube reactor that was glycerine - jacketed. The temperature was controlled by circulating water from a temperature - controlled bath (Polystat, Cole-Parmer, USA). Although the bath contributes to maintain a desired temperature in the samples during sonication, temperature starts to rise because of the rubbing effect of the microtip so that temperature can only be controlled within a range which was 25 - 35ºC or 85 - 93ºC. In order to maintain the temperature within 25 – 35ºC it was necessary to set the bath temperature at 3ºC. When sonication was done on heating at 85 – 93ºC the bath was set at 95ºC. Samples were treated at an amplitude of 20% (114 μm) for 2.5, 5, 10, 12.5, 15 and 20 min maximum.

Light scattering measurements

Mean particle diameter and size distribution were measured using two different equipments depending on the particle size to be measured: (i) between 0.1 – 1000 μm, a Mastersizer 2000E (Malvern Instruments Ltd., UK) was used; equipped with an Hydro 2000 M/MU provided with an He – Ne (633 nm) laser and at a fixed scattering angle of 90º. Refractive index of the disperse phase (1.450) and its absorption parameter (0.001) were used. Droplet size is reported as volume – surface mean diameter or Sauter diameter ($D_{32} = \sum n_i d_i^3 / \sum n_i d_i^2$) where n_i is number of droplets of diameter d_i. D_{32} provides a measure of the mean diameter where most of the particles fall [24,25,26]. (ii) For 0.3 – 6000 nm it was used a ZS Zetasizer Nano (Malvern Instruments Ltd, UK) provided with an He – Ne laser (633nm) and a digital correlator model ZEN 3600. Scattering angle was 173º. Samples were placed in a disposable polystyrene cuvette. The pathlength of the light beam was automatically set by the apparatus, depending from the sample turbidity (attenuation). In dynamic light scattering (DLS), the sample is illuminated with a laser beam and the intensity of the resulting scattered light is dependent of the particle size because of the intensity fluctuations.This technique measures particle diffusion due to Brownian motion and relates this to the particle size. The parameter calculated is defined as the translational diffusion coefficient (D). The particle size is then calculated from the translational diffusion coefficient by using de Stokes-Einstein equation:

$$d(H) = \frac{kT}{3\pi\eta D}$$

where, *d(H)*: hydrodynamic diameter; *D*: translational diffusion coefficient ($m^2\ s^{-1}$); *k*: Boltzmann's constant (1.38×10^{-23} NmK^{-1}); *T*: absolute temperature (K); η: viscosity (N s m^{-2}).

Two approaches were utilized to obtain size information: (i) Contin's algorithm was used to analyze the data for percentile distribution of particle/aggregate sizes[27]. The size

distribution obtained is a plot of the relative intensity of light scattered by particles in various size classes and it is therefore known as an intensity size distribution. Although the fundamental size distribution generated by DLS is an intensity distribution, this can be converted, using Mie theory, to volume distribution; (ii) cumulant method was used to find the mean average (z-average) or the size of a particle that corresponded to the mean of the intensity distribution Z-average is beneficial when citing a single average value with the purpose of comparison, but clearly inadequate for giving a complete description of the distribution results in polydisperse systems.

The average value of ten measurements was reported.

Confocal microscopy

Images were taken using a confocal microscopy (Olympus FV300, UK) provided with an He – Ne laser (543 nm) and objective PLAN APO 60X and 100X. Protein was stained with Rhodamine.

Results and discussion

Effect of US at room temperature on the size and morphology of WPI particles

Figure 1A and 1B shows the mean particle size (D_{32}) and the particle size distribution (% Volume) of the untreated WPI as affected by bulk concentration. A remarkable increase in particle size is noticed when WPI concentration rises from 7.5 to 20 % wt as D_{32} increased from 0.73 ± 0.03 μm to 5.75 ± 0.07 μm. It was already shown for β-lactoglobulin that at a fixed temperature and pH, the size of aggregates depends on concentration [28]. Boulet et al. (2000) have already described this phenomenom for whey

protein, soybean protein and casein showing that above a transition concentration of 0.04 – 0.07 ml/ml, depending on the nature of the protein, pH and ionic strength, aggregation increased in log relationship with increase of volume concentration. They suggested that subparticles may be involved in the formation of the particles and that diluting to infinity may reveal their size. Subparticles would be formed from a limited number of protein molecules through hydrophobic interactions and hydrogen – bonding. These subparticles would exhibit a characteristic compact quaternary structure but large aggregates would be formed, beyond a critical size or protein concentration, by the association of subparticles into voluminous and open clusters. Growth of the particle takes place by means of local surface electrostatic charges attraction, moreover non elastic particle – particle collision may reduce the diffusion coefficient and give apparent larger diameter at high than low concentrations but this effect is relatively small with Newtonian dispersions [29]. Figure 1B shows that at the lowest concentration (7.5 %wt), the particle size distribution was polimodal with three representative peaks: the higher one showed a particle size variation between 0.1 and 3 μm; the other two peaks showed a diameter range between 3 and 20 μm, and 50 and 500 μm. As WPI concentration increased (9, 12, 15 and 20 % wt), all the three peaks decreased and an almost monomodal distribution with a size diameter between 50 and 500 μm was obtained at concentrations higher than 9 %wt. Increasing intensity of this peak in the range 12 – 20 % wt WPI accounts for by big rise of mean diameter observed in Figure 1A.

First of all we studied how US affected the size of WPI when applied avoiding temperature effects. Figure 2A shows that the particles size of WPI 7.5 % wt decreased under the effects of ultrasound. Particles showed a great decrease in size during the first 2 min of sonication, from 0.73 ± 0.03 μm to 0.359 ± 0.005 μm and leveled off after 5

min sonication. Sonicated samples showed monomodal particle size distributions (% Intensity) (Figure 2B) with slight differences for 2, 10 and 20 min of sonication and a broad diameter range (from 0.1 to 1 μm), which is very different from the distribution of the untreated sample in Figure 1B. The sonication technique for size reduction has been proposed in many studies, as for breakage of agglomerated sugar crystals (20 kHz, amplitudes between 41 and 61%, for 5 min at 25ºC) noticing that at higher amplitudes less agglomerates are left in the sample [22]. More recently for size reduction on soy protein isolates and concentrates (15 min sonication with a frequency of 20 kHz [26]).

The results in Figure 2 are in agreement with the observations performed by confocal microscopy (Figures 3A and B). Figure 3A reveals the great polydispersity of untreated 7.5 %wt WPI with big and small particles with heterogeneous shapes. After 10 min sonication (Figure 3B) the surface of the particles became smoothed. In addition, many small particles are formed as a result of the breakup of the large ones. The chances of being attacked by the cavitation energy increases with increasing molecular weight species and may be because smaller molecular weight species have shorter relaxation times and, thus, can resist the sonication stress more easily [17]. Similar spherical shapes were found for sonicated tin nanoparticles [21] and silica particles [3].

Increasing WPI concentration to 12 % wt the mean diameter also decreased after 10 min sonication at room temperature (Figure 4, curve B and C). Figure 5 shows that 12 and 7.5 % wt WPI showed a similar monomodal size distribution with $Z_{average}$ of 0.428 and 0.216 μm respectively after 10 min sonication.

Effect of US at room temperature on the size and morphology of WPI gelled particles

WPI dispersions (9 – 20 % wt) were gelled at 80ºC for 30 min and diluted 1:1 in water. WPI gel concentration had a strong impact on the mean size of gel particles as shown in Figure 6. For sonication studies we selected a gel of 15 % WPI with initial mean particle size of 87 ± 3 μm. Nevertheless, the effective concentration for this sample during sonication was 7.5 % wt due to dilution as mentioned above. The size reduction was greater during the first minutes of sonication (2.5 min), when agglomerates were bigger (Figure 7A) reaching a mean size of 6.90 ± 0.01 μm. Size reduction was accelerated between 10 and 12.5 min (D_{32} decreased from 4.88 ± 0.03 to 1.61 ± 0.01 μm). After then, size reduction was less abrupt.

Particle size distribution for non sonicated gelled WPI dispersion (Figure 7B) was monomodal with significant span values (from 50 to 1000 μm). At 2.5 min and up to 10 min sonication was also monomodal but with a narrower size range (5 – 50 μm for 2.5 min sonication and 2 – 20 μm for 10 min). After 10 min sonication a second lower size peak between 0.1 and 1 μm appeared because of reduction of particles comprised within 2 and 20 μm. The formation of submicron particles accounts for by the acceleration in size reduction observed in Figure 7A after 10 min sonication.

A similar behavior with sonication time was shown when disrupting water soluble corn hull heteroxylan. The viscosity decreased first rapidly and then slowly with time and reached a constant value corresponding to a minimum below which the polysaccharide chains no longer break [30]. This effect was also found when sonicating dickite dispersions. The proportion of the smallest particles (0.5 μm) increased sharply with sonication, and at the same time the modal size of the greatest ones (12 μm) was progressively decreased to 3.8 μm after 20 hs of treatment [23].

Figure 8 shows the confocal microscopy image of particles obtained after 10 min sonication of gelled WPI (15 %wt). The size agrees with the mean size or distribution

determined by light scattering (Figure 7). However, it was observed a tendency to flocculation that deserves further investigation.

Effect of US under heating WPI on the size and morphology of particles

As shown above, sonication produced a marked reduction in particle size. Contrarily, heating of WPI solutions leads to an increase of particle size by aggregation of proteins. Because of the opposite effects of these treatments it seems possible to control the size of WPI particles by simultaneous heating and sonication. In Figure 4 (line A) it is shown that when heating at 85–93ºC WPI solutions under sonication (10 min), the particle size was reduced for the lowest WPI concentration (7.5 %wt), did not change at 9 % wt but strongly increased at 12 % wt in comparison with the untreated sample (line B). In the particular case of WPI 7.5 %, the resulting particle size (line A) was smaller than the mean diameter of untreated WPI (line B) suggesting that the disrupting effect of sonication predominated over heat-aggregation. However, at 12 % WPI the effect of protein aggregation due to heating prevailed over the disrupting effect of sonication; particle size was 2.02 ± 0.01 μm and 4.50 ± 0.01 μm for untreated and heat-sonicated WPI, respectively.

Figure 9 shows the size distribution of those samples after sonication under heating. Size distribution has a wide polydispersity for all concentrations. The broader corresponded to WPI 12 %wt and it ranged from 0.5 to 500 μm. For 9 and 7.5 % wt polydispersity was smaller (0.1 – 10 μm for 9% and 0.1 – 8 μm for 7.5 %) taking in consideration only the largest peak for each one of them. Confocal microscopy (Figure 10) corroborated the particles size distribution shown in Figure 9, as a high polidispersity was observed.

This study shows that WPI particles of desired size may be obtained either by sonication of gelled WPI or by sonication under heating at denaturation temperature. As an example, WPI particles of similar mean diameter (4.5 μm) can be obtained by sonication of gelled 15 % WPI or by heating and simultaneous sonication of 12 % wt WPI. However, a more polydisperse size distribution is apparent for the last procedure (Figure 11).

Conclusions

High intensity ultrasounds are an effective technique to control size and shape of protein particles within the micronic range. An accurate selection of the process variables allows to control the mean size as well as the polydispersity or even the shape of protein particles.

References

1. J. Mc Clements, Advances in the application of ultrasound in food analysis and processing. Trends in Food Science and Technology. **6**, 293 – 299 (1995).
2. D. Knorr, M. Zenker, V. Heinz, Dong – Un Lee, Application and potential of ultrasonics in food processing. *Trends* in Food Science & Technology. **15**, 261 – 266 (2004).
3. Y. F. Lu, N. Riyanto, L. K Weavers, Sonolysis of synthetic sediment particles: particle characteristics affecting particle dissolution and size reduction. Ultrasonics Sonochemistry. **9**, 181 – 188 (2002).

4. J. Klíma, A. Frias – Ferrer, J. González – García, J. Ludvík, , V. Saéz, J. Iniesta, Optimisation of 20 kHz sonoreactor geometry on the basis of numerical simulation of local ultrasonic intensity and qualitative comparison with experimental results.Ultraosnics Sonochemistry. **14,** 19 – 28 (2006).
5. C. Horst, Y. S. Chen, U. Kunz, U. Hoffmann, Design, modeling and performance of a novel sonochemical reactor for heterogeneus reactions. Chemical Engineering Science, **51**, 1837 – 1846 (1996).
6. T. G. Leighton, Bubble population phenomena in acoustic cavitation. Ultrasonics Sonochemistry. **2**, No. 2, S123 – S136 (1995).
7. M.Villamiel, P. Jong, Influence of High – Intensity Ultraosund and Heat Treatment in Continuous Flow on Fat, Proteins and Native Enzymes of Milk. Journal of Agricultural and Food Chemistry. **48**, 472 – 478 (2000).
8. F. Priego – Capote, M. D. Luque dr Castro, Analytical uses of ultrasound I. Sample preparation. Trends in Analytical Chemistry. **23**, No. 9, 644 – 653 (2004).
9. Sujata Hena, H.Das, Modeling of particle size distribution of sonicated coconut milk emulsion: Effect of emulsifiers and sonication time. Food Research International. **39**, 606 – 611 (2006).
10. S. Freitas, B.Rudolf, P. M Hans, B.Gander, Flow – through ultrasonic emulsification combined with static micromixing for aseptic production of microspheres by solvent extraction. European Journal of Pharmaceutics and Biopharmaceutics. **61**, 181 – 187 (2005).
11. J. Pereira – Lachataignerais, R. Pons, P. Panizza, L.Courbin, J. Rouch, O. López, Study and formation of vesicle systems with low polydispersity index by ultrasound method. Chemistry and Physics of Lipids. **140**, 88 – 97 (2006).

12. J. P. Lorimer, T. J. Mason, T. C. Cuthbert & E. A. Brookfield, Effect of ultrasound on degradation of aqueous native dextran. Ultrasonics Sonochemistry. **2,** s55 – s57 (1995).

13. R. H. Chen, J. R. Chang & J. S. Shyur, Effect of ultrasounds conditions and storages in acidic solutions on changes in molecular weight and polydispersity of treated chitosan. Carbohydrate Research. **299**, 287 – 294 (1997).

14. N. Kardos & J. Luche, Sonichemistry in carbohydrate compounds. Carbohydrate Research. **332**, 115 – 131 (2001).

15. R. Eschette, D. P. Norwood, Ultrasonic degradation of polysaccharides studied by multiangle laser light scattering. Presented as a poster number RI – 107 at the Annual March Meeting of the Physical Society. Austin, TX, USA, March 3 – 7 (2003).

16. H. Liu, J. Bao, Y. Du, X. Zhou & J. F. Kennedy, Effect of ultrasonic treatment on the biochemphysical properties of chitosan. Carbohydrates Polymers. **64**, 553 – 559 (2006).

17. Y. Iida, T. Tuziuti, K. Yasui, A. Towata & T. Kozuka, Control of viscosity in starch and polysaccharide solutions with ultrasound after gelatinization. Innovative Food Science & Emerging Technologies. **9**, 140 – 146 (2008).

18. N. Camino, O. E. Pérez, A. M. R. Pilosof, Molecular and functional modification of hydroxypropylmethylcellulose by high - intensity ultrasound. Food Hydrocolloids. **23**, 1089 – 1095 (2009).

19. Z. Xiaodong, L. Qunfang, D. Gance & J. Faxiangb, Ultrasonic degradation of polysilane polymers. Polymer degradation and stability. **60**, 409 – 413 (1998).

20. I.Gülseren, D. Güzey, B. D. Bruce & J. Weiss, Structural and functional changes in ultrasonicated bovine serum albumin solutions. Ultrasonic Sonochemistry, **14**, 173 – 183 (2007).

21. Z. Li, X. Tao, Y. Cheng, Z. Wu, Z. Zhang, H. Dang, A facile way for preparing tin nanoparticles from bulk via ultrasound dispersion. Ultrasonics Sonochemistry. **14**, 89 – 92 (2007).

22. Z. Guo, A. G. Jones, N. Li, S.Germana, High – speed observation of the effect of ultraosund on liquid mixing and agglomerate crystal breakage processes. Powder Technology. **171**, 146 – 153 (2007).

23. F. Franco, J. A. Cecila, L. A. Pérez – Maqueda, J. L. Pérez – Rodriguez, C. S. F.Gomes, Particle – size reduction of dickite by ultrasound treatments: Effect on the structure, shape and particle – size distribution. Applied Clay Science. **35**, 119 – 127 (2007).

24. X. Huang, Y. Kakuda, W.Cui, Hydrocolloids in emulsions: particle size distribution and interfacial activity. Food Hydrocolloids, **15**, 533- 542 (2001).

25. J. Leroux, V. Lagendorff, G. Schick, V. Vaishnav, J. Mazoyer, Emulsion stabilizing properties of pectins. Food Hydrocolloids. **17**, 455 – 462 (2003).

26. Jambrak, V. Lelas, T. Mason, G. Kresic, M. Badanjak, Physical properties of ultrasound treated soy proteins. Journal of Food Engineering. **93**, 386 – 393 (2009).

27. P. Stepanek, Dynamic light scattering: the method and some applications, W. Brown ed.; Oxford University Press. 177 (1993).

28. V. Militello, C. Cassarino, A. Emanuele, A.Giostra, F. Pullara, M. Leone, Aggregation kinetics of bovine serum albumin studied by FTIR spectroscopy and light scattering. Biophysical Chemistry, **107**, 175 – 187 (2004).

29. M. Boulet, M. Britten, F. Lamarche, Aggregation of some food proteins in aqueus dispersions: effect of concentration, pH and ionic strength. Food Hydrocolloids. **14**, 135 – 144 (2000).

30. Ebringerová, Z. Hromádková. The effect of ultrasound on the structure and properties of the water soluble corn hull heteroxylan. Ultrasonics Sonochemistry. **4**, 305 – 309 (1997).

Legends for figures

Fig. 1: Effect of WPI concentration on particle size. (A) mean diameter D_{32} and (B) particle size distribution, of WPI 7.5%, 9%, 12%, 15% and 20 % wt.

Fig. 2: Effect of sonication time at 25-35 ºC on particle size for WPI 7.5 % wt. (A) mean diameter $Z_{average}$ and (B) particle size distribution at 2, 10 and 20 min.

Fig. 3: Confocal microscopy images of WPI 7.5 % for (A) untreated WPI (D_{32} = 0.74 ± 0.03 µm) and (B) after 10 min sonication at 25-35 ºC ($Z_{average}$ = 0.216 ± 0.003 µm).

Fig. 4: Effect of WPI concentration on the mean particle size. For: (A) 10 min sonication on heating at 85–93°C, (B) untreated WPI and (C) 10 min sonication at 25-35 ºC.

Fig. 5: Particle size distribution of (A) 7.5 % wt and (B) WPI 12 % wt, after 10 min sonication at 25-35 ºC.

Fig. 6: Effect of WPI concentration on particle size of WPI gels heated at 80°C for 30 min.

Fig. 7: Effect of sonication time on particle size of gelled WPI (15 % wt). (A) mean size D_{32} and (B) particle size distribution, after 0, 2.5, 10, 12.5 and 20 min sonication at 25-35 ºC.

Fig. 8: Confocal microscopy images of particles after 10 min sonication at 25-35 ºC of gelled WPI (15 % wt). (D_{32}= 4.88± 0.03 µm).

Fig. 9: Particle size distribution for WPI 7.5%, 9% and 12 % wt after 10 min sonication on heating at 85–93°C. (D_{32} = 0.482 ± 0.001, 0.97 ± 0.05, 4.50 ± 0.01 µm, respectively).

Fig. 10: Confocal microscopy images of particles after 10 min sonication on heating at 85–93°C (A) WPI 7.5 % (D_{32} = 0.482 ± 0.001µm) and (B) WPI 12 % wt (D_{32} = 4.5 ± 0.1 µm).

Fig. 11: Comparison of two procedures to obtain particles of approximately 4.5 µm. (A) 10 min sonication at 25-35 ºC of gelled WPI (15 % wt) and (B) 10 min sonication on heating at 85–93°C of WPI (12 % wt).

Figure 1

Click here to download Figure: Fig.1.docx

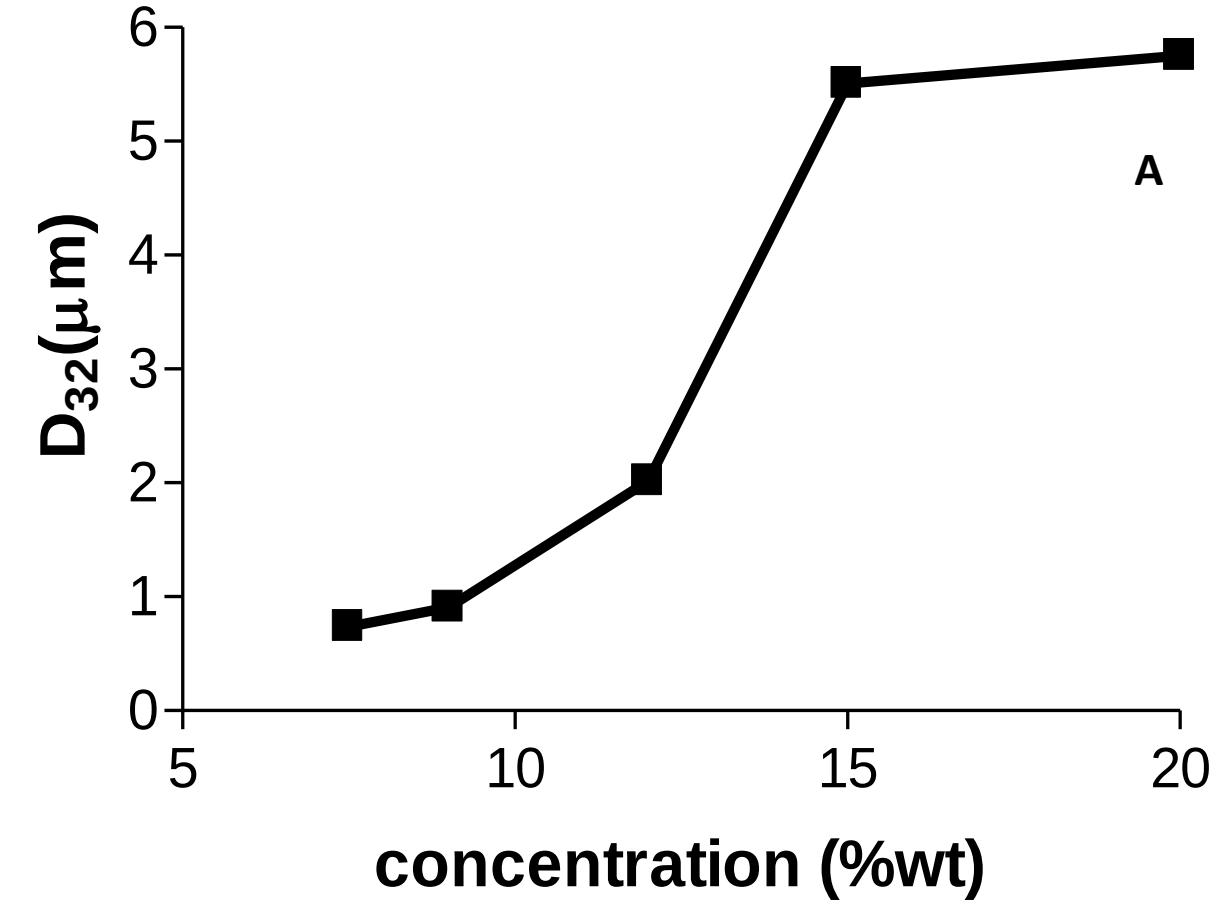

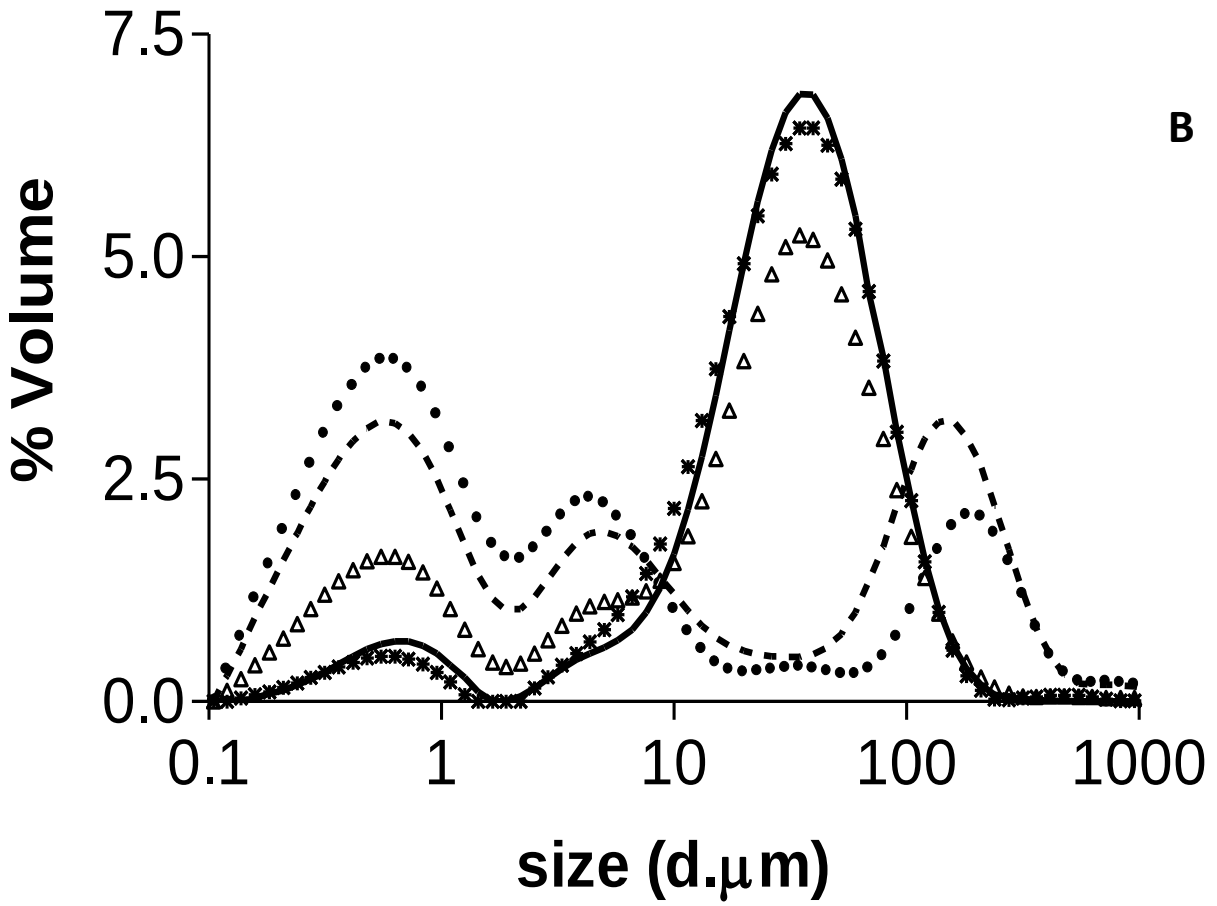

Figure 1

Figure 2

Click here to download Figure: Fig.2.docx

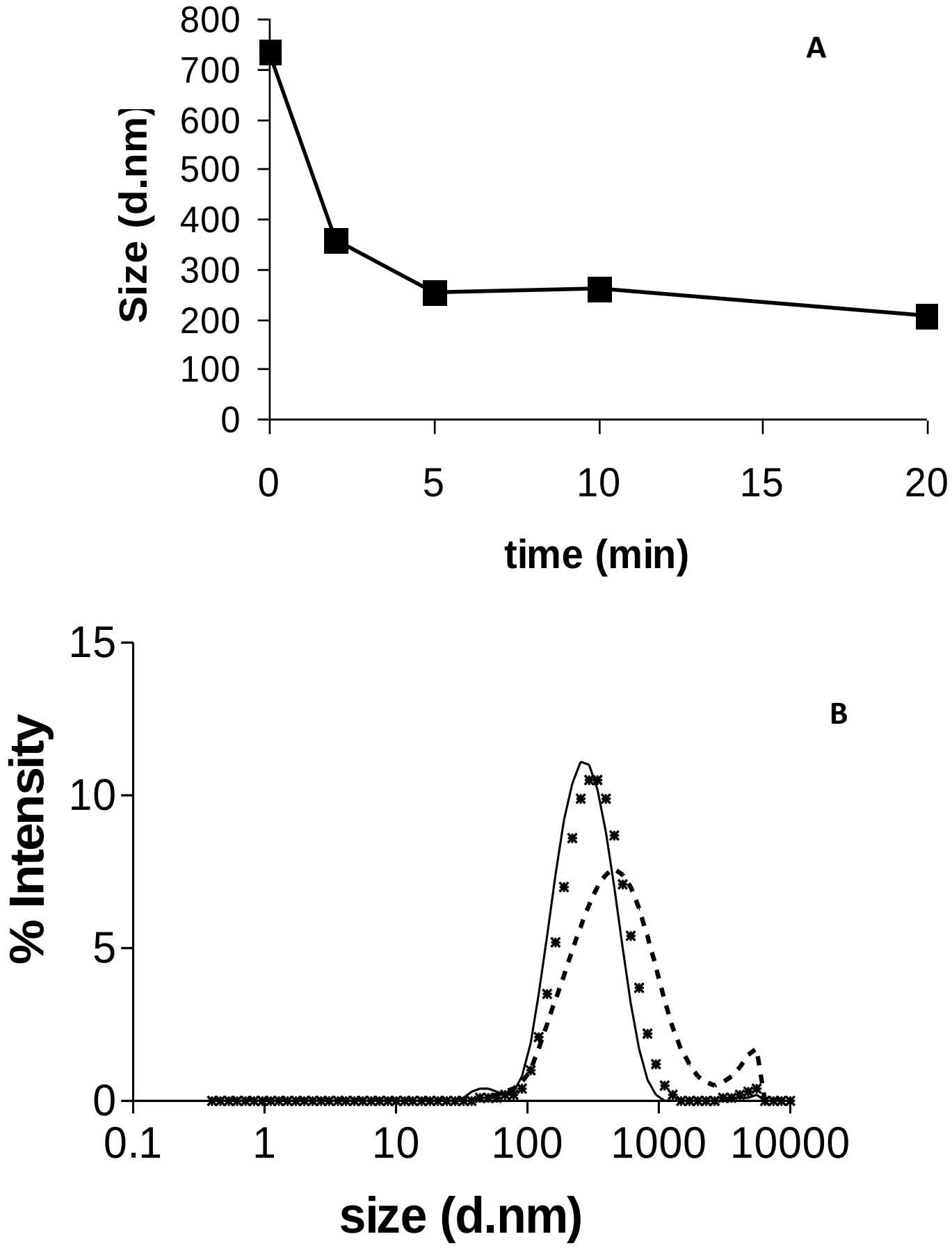

Figure 2

Figure 3

Click here to download Figure: Figc3.docx

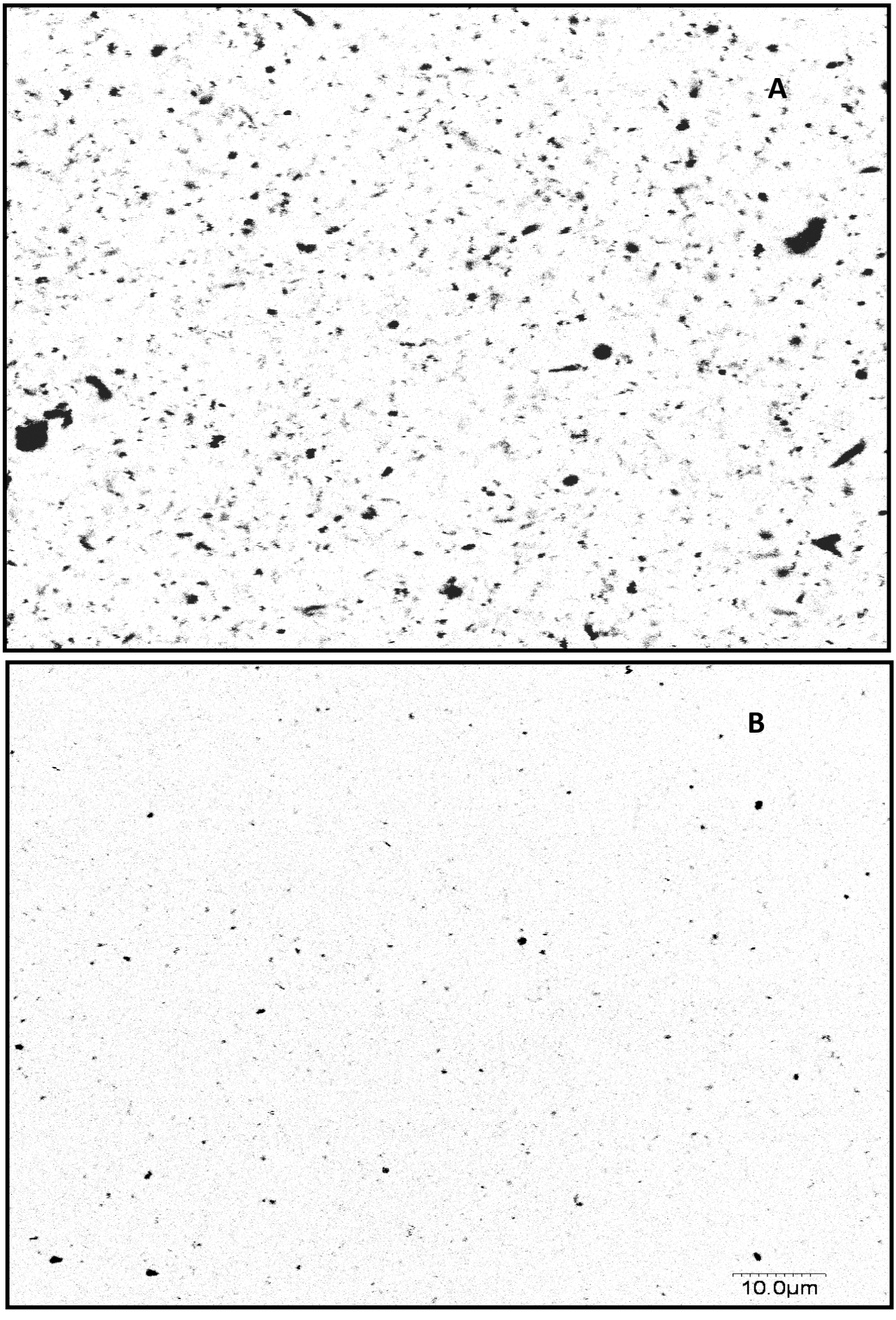

Figure 3

Figure 4

Click here to download Figure: Fig.4.docx

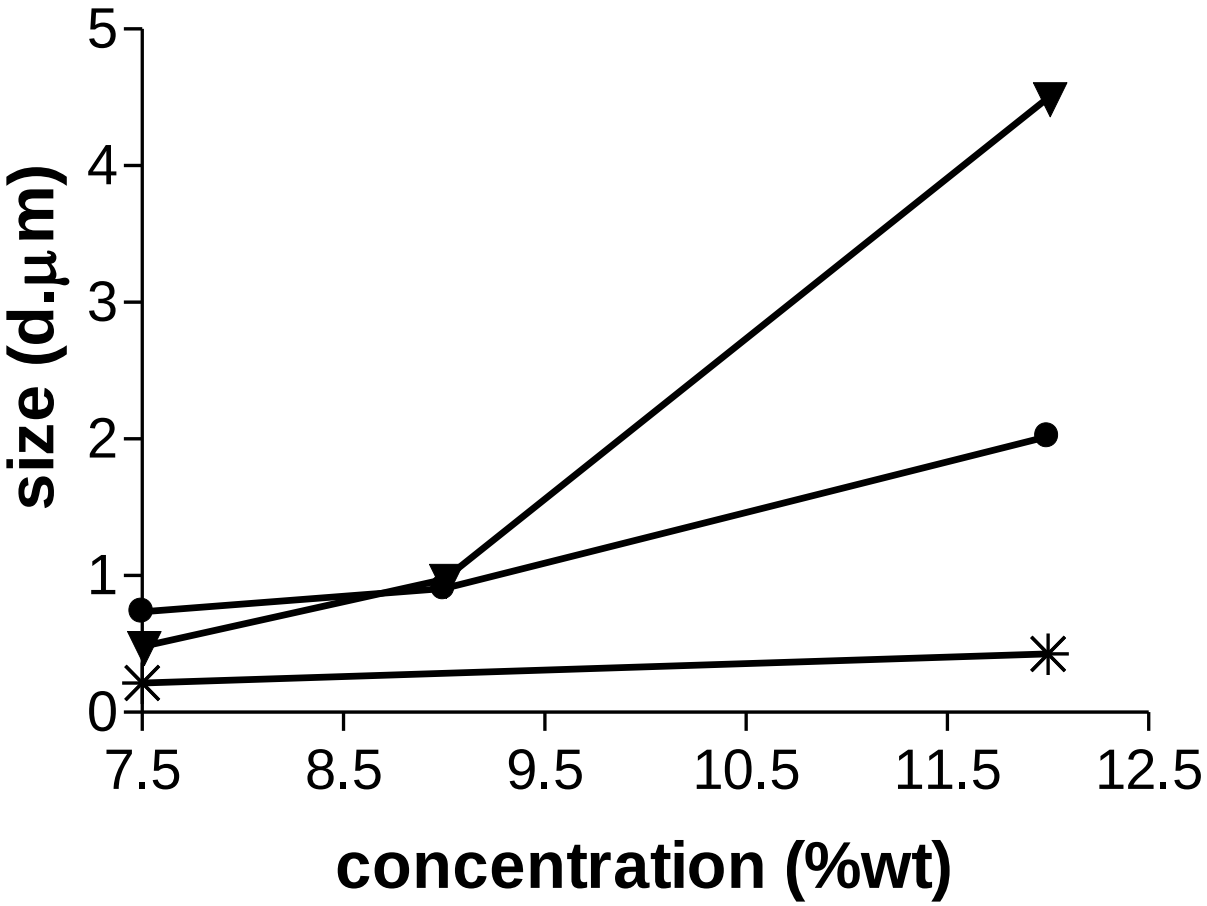

Figure 4

Figure 5

Click here to download Figure: Fig.5.docx

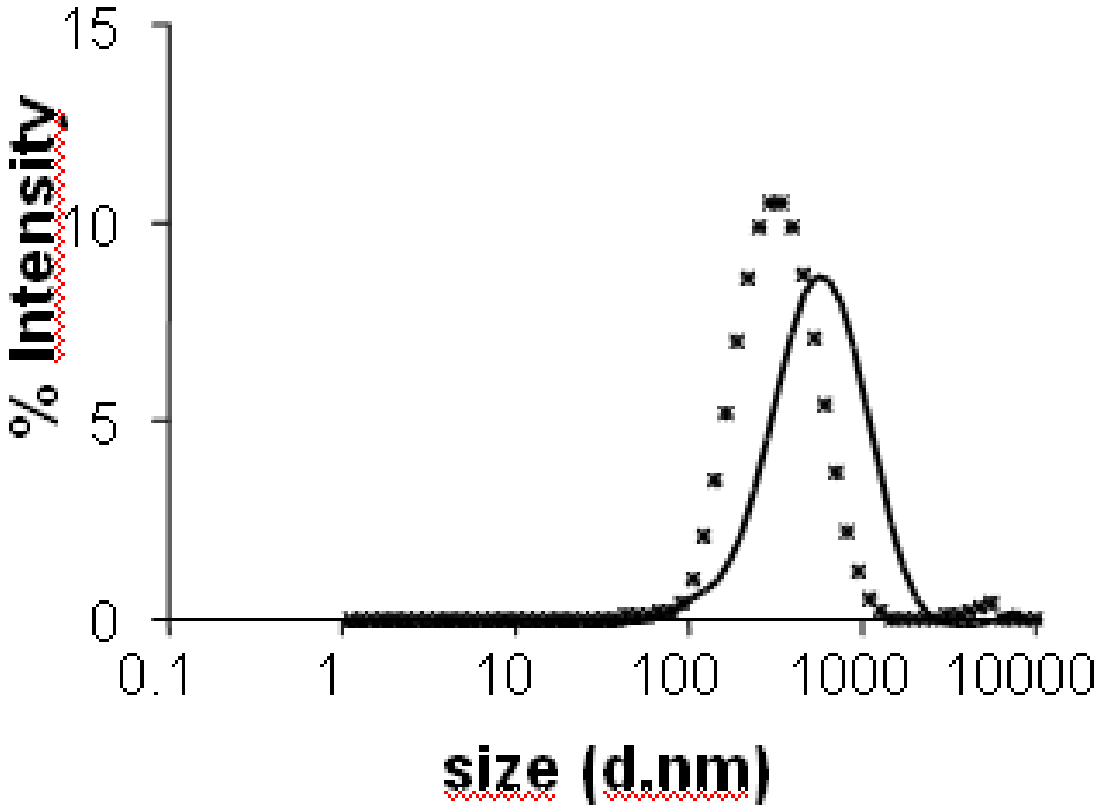

Figure 5

Figure 6
Click here to download Figure: Fig.6.docx

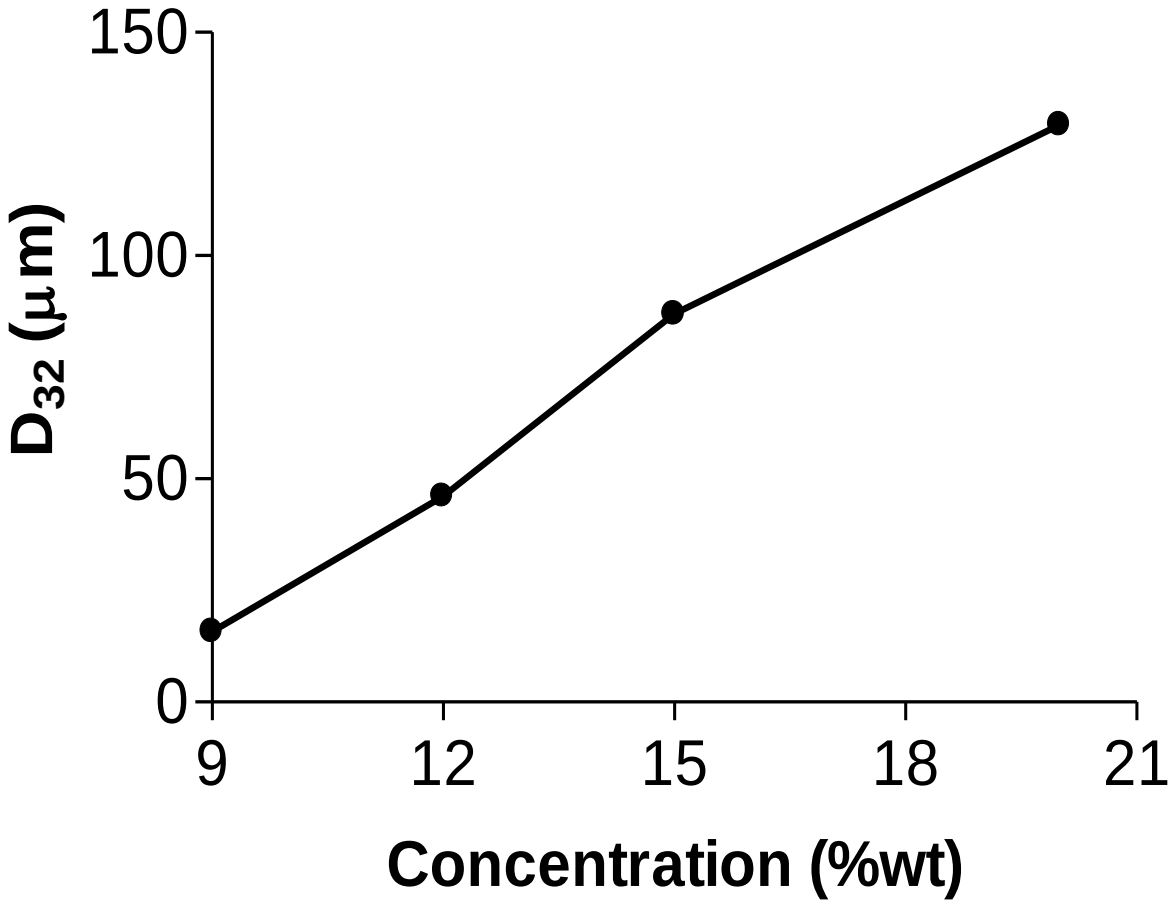

Figure 6

Figure 7

Click here to download Figure: Fig.7.docx

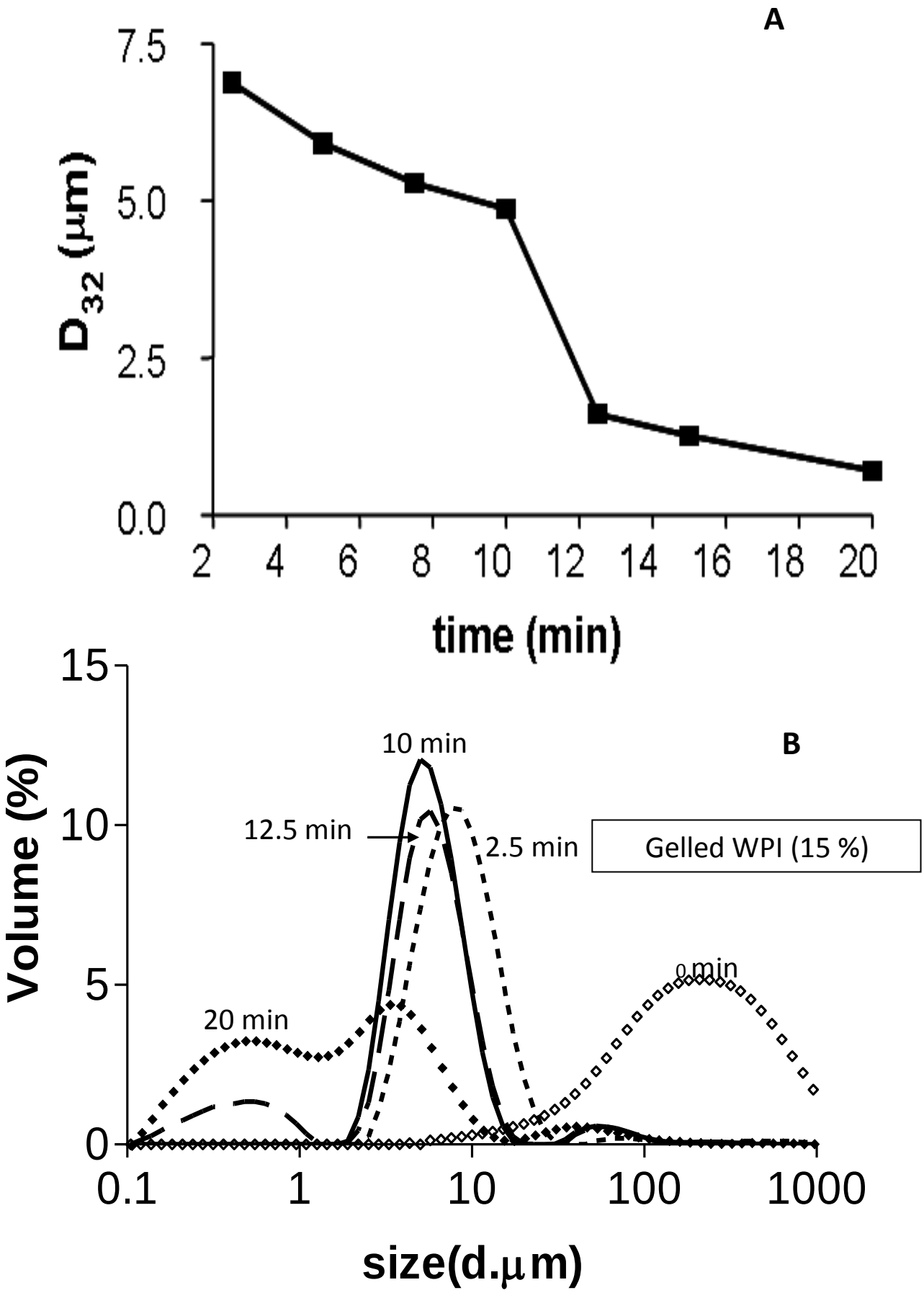

Figure 7

Figure 8

Click here to download Figure: Fig.8.docx

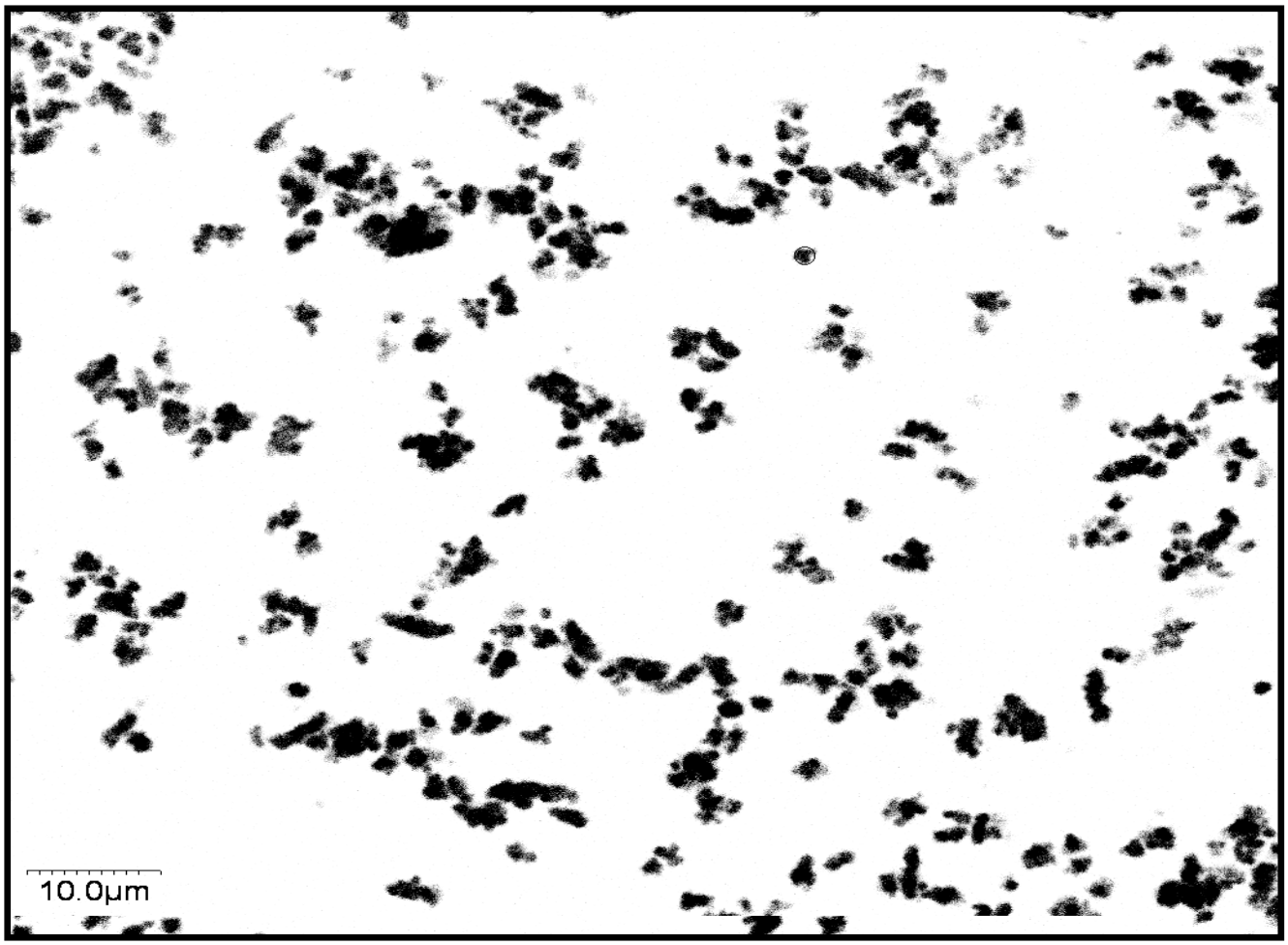

Figure 8

Figure 9
Click here to download Figure: Fig.9.docx

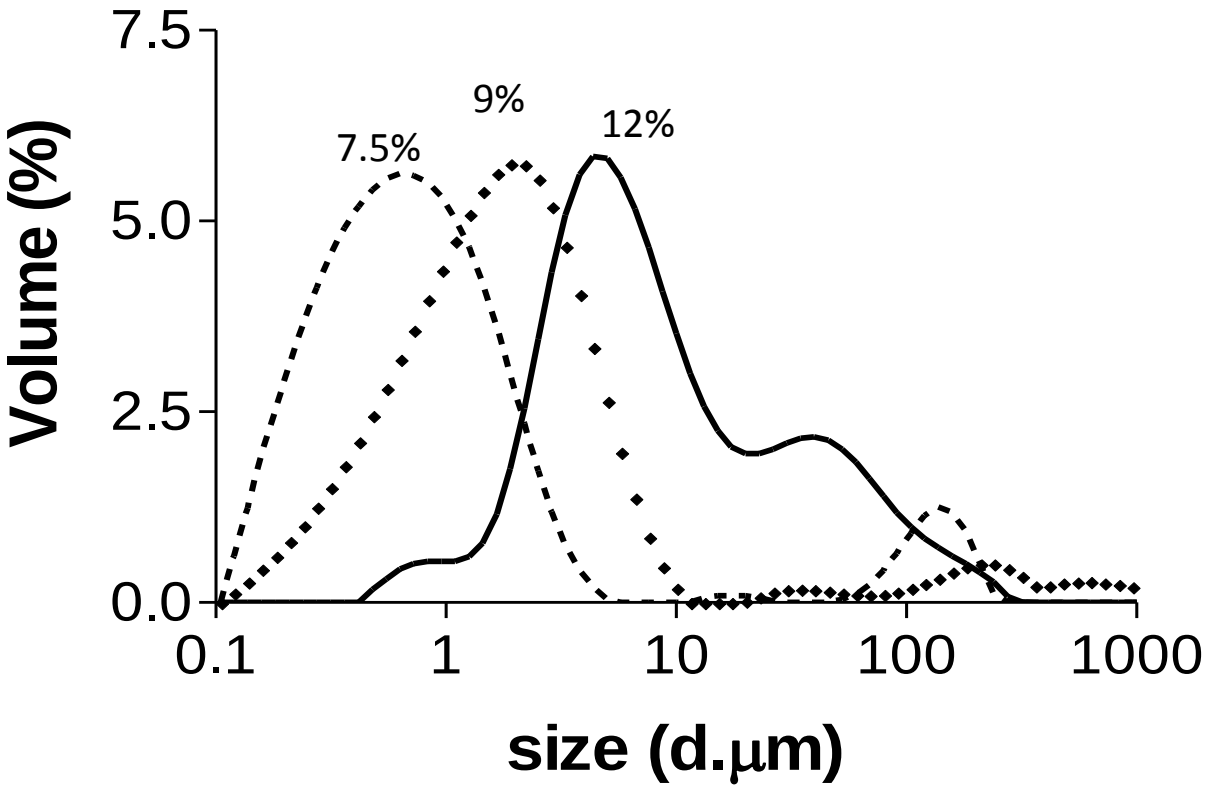

Figure 9

Figure 10

Click here to download Figure: Fig.10.docx

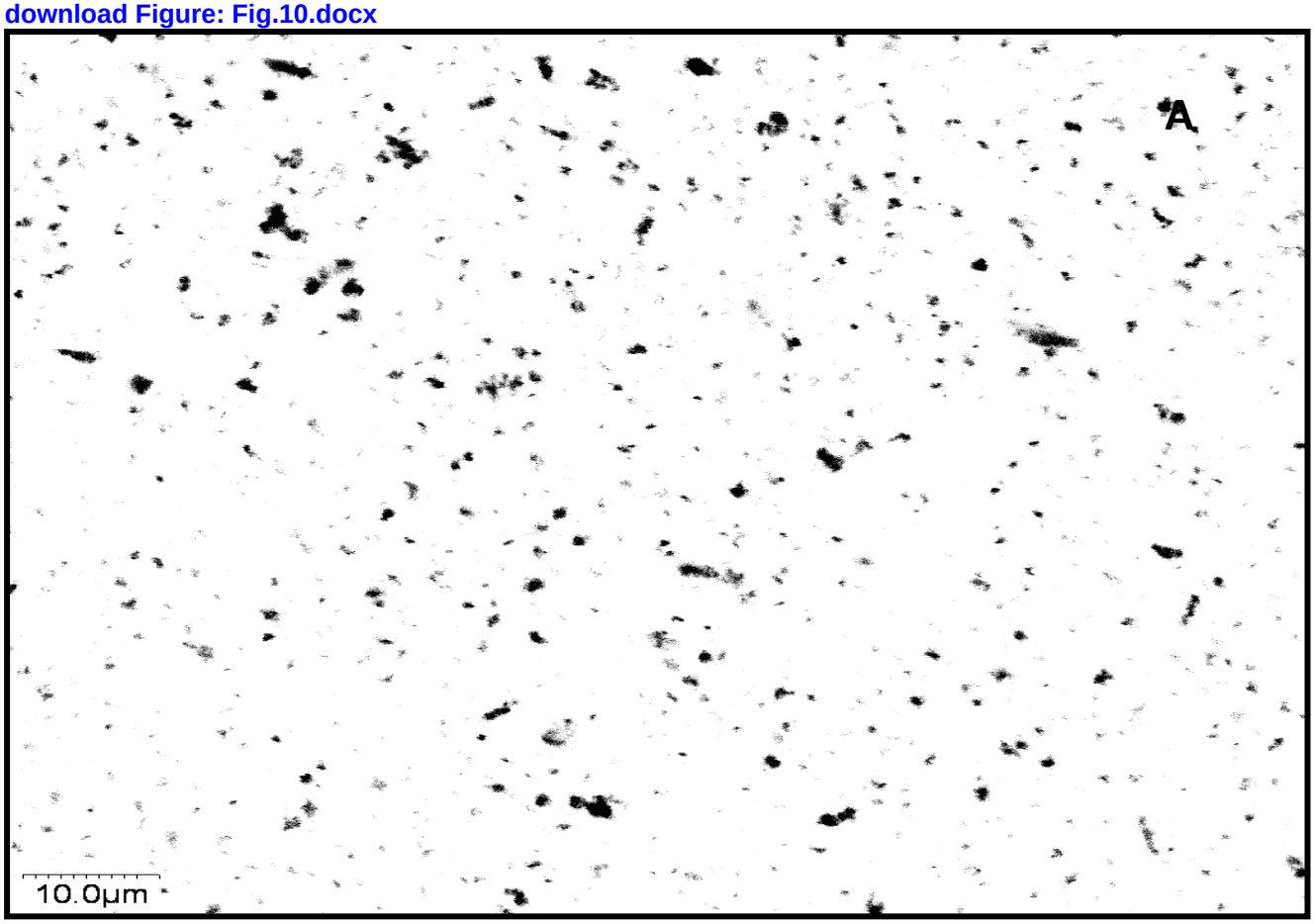

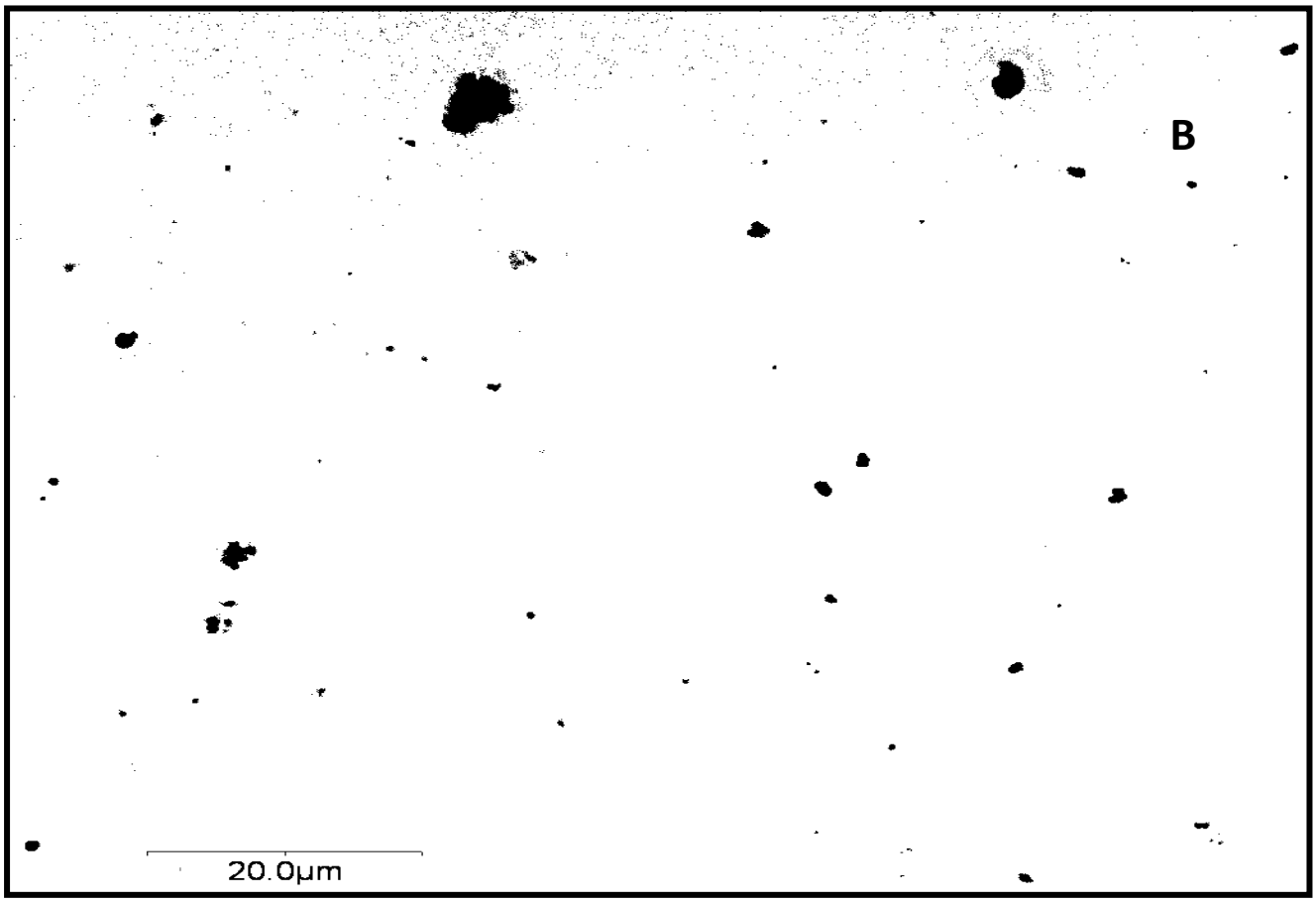

Figure 10

Figure 11
Click here to download Figure: Fig.11.docx

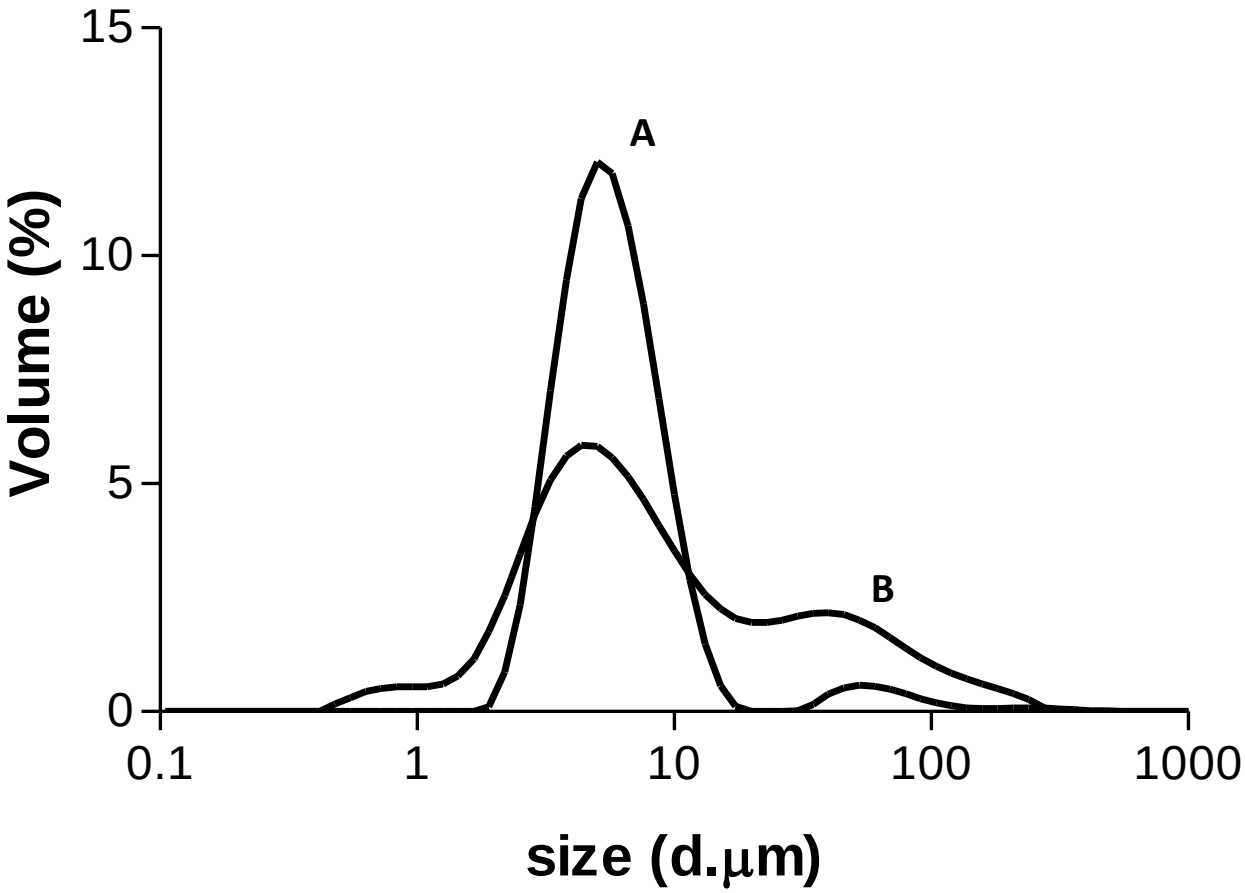

Figure 11